

A Novel Optical Gate by Integration of a Photodiode and an Electroabsorption Modulator*

Liao Zaiyi[†], Pan Jiaoqing, Zhou Fan, Bian Jing, Zhu Hongliang, Zhao Lingjuan, and Wang Wei

(Key Laboratory of Semiconductors Materials, Institute of Semiconductors, Chinese Academy of Sciences, Beijing 100083, China)

Abstract: A compact and stable three-port optical gate has been successfully fabricated by monolithically integrating a simple photodiode and an electroabsorption modulator. The gate shows an excellent DC logic “and” function with different load resistors. Its dynamical characteristics without packaging have also been measured. We observed a dynamic extinction ratio of over 7dB with a 950Ω load resistor and a 7mW control light power at 622Mbit/s.

Key words: electroabsorption modulator; photodiode; monolithic integration

EEACC: 4150; 4180; 4270

CLC number: TN491

Document code: A

Article ID: 0253-4177(2008)05-0898-05

1 Introduction

Ultra-fast optical gates will be the key devices for the next generation of optical communications because of their flexible application in optical signal processing, such as DEMUX, 2R regeneration, wavelength conversion, and so on. Compared with “all-optical” type optical signal processes such as cross-gain modulation (XGM), cross-absorption modulation (XAM), and cross-phase modulation (XPM)^[1], the traditional optical-electronic-optical (O-E-O) process is mature and stable. But the signal is amplified and processed in the electrical region, which is complicated and costly. Recently, a novel photodiode (PD) and modulator O-E-O gate was suggested. Figure 1 shows

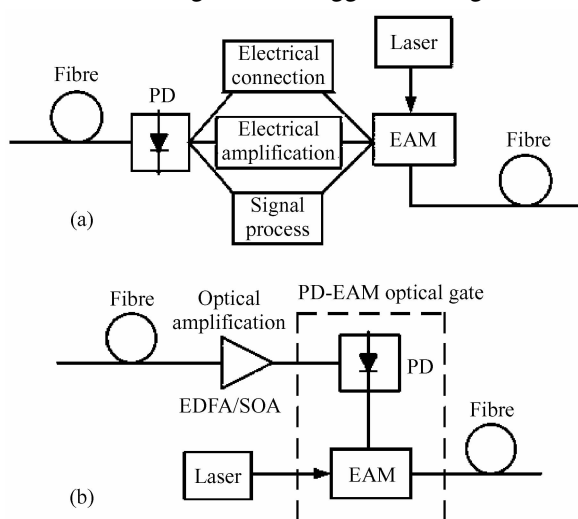


Fig.1 (a) Diagram of the traditional O-E-O signal process; (b) Diagram of the signal process based on a PD-EAM optical gate

configurations of the optical signal process based on traditional O-E-O conversion and a PD-EAM optical gate. First, the optical signal is amplified by EDFA or SOA, and then the signal is converted into an RF signal to drive EAM directly through a high output PD. This demonstrates compact configuration and high speed-operation capacity due to short electrical interconnects and release of electrical amplification. The very short open gate time of 2.3ps for this optical gate has been demonstrated and used in optical signal processes^[2~5]. But, the optical power consumption is very large and detailed reports are rare. A low optical consumption gate is also reported in the GHz-range with an optical wavelength-converting switching of only ~10mW of absorbed input optical power^[6]. In this letter, a low power PD-EAM optical gate is designed and fabricated and its characteristics are tested in a 622Mbit/s system.

2 Principle and design

Figure 2 shows a circuit diagram of the PD-

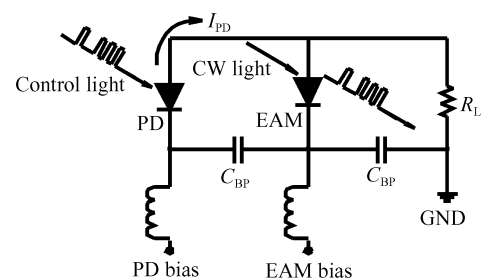


Fig.2 Circuit diagram of a PD-EAM optical gate and illustration of its operation

* Project supported by the National Natural Science Foundation of China (No.90401025)

[†] Corresponding author. Email: lzy1348@semi.ac.cn

Received 4 September 2007, revised manuscript received 17 November 2007

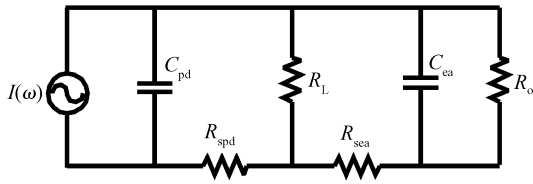


Fig.3 Radio frequency model of a PD-EAM optical gate

EAM. It contains a surface-illuminated InGaAs photodiode, a multi-quantum wells (MQW) EAM, and a thin-film resistor, which were monolithically integrated on Fe-InP chip. Two bias-Ts consisting of a bypass capacitor and an inductor provide DC voltage for the EAM and PD and confine all RF electrical signals in the area very close to InP chip. The principle and operation process of the PD-EAM optical gate are as follows:

First, the control light and the continuous light are coupled into the PD and one port of the EAM separately. The signal light is output from the other port of the EAM. Second, the EAM bias adjusts to ensure the MQW heavily absorb the continuous light. So, the output signal beam is weak and the optical gate's state is "Off". Third, when the peak of the control light with the coded signal illuminates the PD, an electrical photocurrent (I_{pd}) is generated and flows through the load resistor (R_L) into ground, which creates a voltage drop across the resistor and reduces EAM reverse bias voltage. This drop can decrease MQW absorption. If the control light peak power is large enough, the MQW is nearly transparent to continuous light at this time. As the result, the optical gate's state is "On".

As an optical gate, some crucial parameters should be considered.

(1) Insertion loss. Insertion loss of the PD-EAM optical gate is the same as that of EAM. It can be decreased below 5dB by elaborately designing the EAM waveguide with a spot-size-converter (SSC)^[7].

(2) Extinction ratio (ER). Defined as the on-state and off-state power ratio of the optical gate, it is the same as the EAM:

$$ER_{dB} = 4.343\Gamma_{MQW}\Delta\alpha L \quad (1)$$

where $\Delta\alpha$ is related to the absorptive character of the MQW and the voltage swing across the EAM junction.

(3) Bandwidth. The equivalent RF electrical model is shown in Fig. 3, where $I(\omega)$ is the RF source generated by PD, C_{pd} and C_{ea} represent junction capacitances of PD and EAM, respectively; R_{spd} and R_{sca} represent the contact resistance of PD and EAM, respectively. Some parasitic capacitance and inductance are ignored here, but the photocurrent in an EAM

must be carefully discussed. Suppose the photocurrent is a current path rather than a current source. The current value varies with junction voltage, so it can be modeled by a resistance $R_o = (dI_o/dV_J)^{-1}$, where I_o is the EAM DC photocurrent and V_J is the junction voltage. The 3dB electrical bandwidth is approximately:

$$f_{3dBc} = \sqrt{3}/2\pi R_{eff}(C_{pd} + C_{ea}) \quad (2)$$

where $R_{eff} = R_o // R_L$.

(4) Power consumption. When PD and EAM work in reverse bias, electrical consumption is low due to their small working current. The power of the control light needs to be large to generate enough electrical RF signal to drive the EAM in order to achieve certain ER. The voltage swing across the EAM junction is:

$$\Delta V_{ea} = R_{PD} P_{control} R_{eff} \quad (3)$$

where R_{PD} is the responsivity of PD, $P_{control}$ is the power of the control light, and R_{eff} is related to R_L and R_o .

Accounting for key parameters of PD-EAM, design guidelines can be obtained from Eq. (1) to Eq. (3). In order to design a high speed, low insertion loss, low optical power consumption optical gate, the PD and EAM are optimized separately. From Eq. (1), $\partial\alpha/\partial V_{ea}$ of the EAM must be enlarged to achieve low drive voltage and decrease insertion loss. From Eq. (3), the PD must be designed to obtain larger responsivity and higher saturated output power. From Eq. (2), the size of the PD and EAM must be reduced to decrease junction capacitance and obtain large bandwidth. Choosing a proper R_L is complicated because a small R_L can enhance bandwidth, but needs a higher control light power. In order to reduce the power of the control light, $R_L = 950\Omega$ in a 622Mbit/s system is chosen.

3 Material epitaxy and device fabrication

An illustration of the PD-EAM optical gate is shown in Fig. 4. The device needs two metal-organic vapor phase epitaxy (MOVPE) growth processes. The EAM structure is grown on Fe-InP substrate first, and the EAM epitaxy layer in the PD area is selectively etched with SiO_2 as an etching mask. The PD is grown on to the PD area after carefully cleaning the wafer surface. For the electro-absorption modulator we employed, the QCSE rather than the Franz-Keldysh effect for MQW provides stronger change in absorption caused by the EAM junction voltage change ($\partial\alpha/\partial V_{ea}$). The MQW consists of 10 1.57Q-InGaAsP wells (9nm thick, 0.4% tensile strain) with 1.2Q-InGaAsP

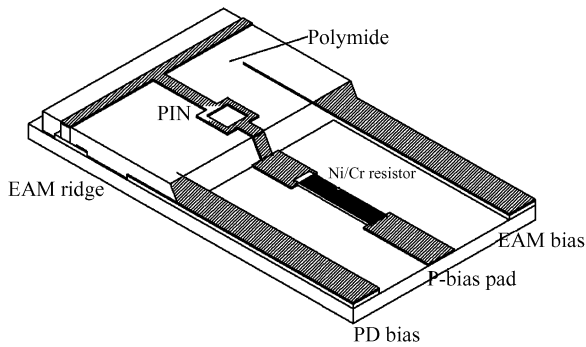


Fig. 4 Illustration of a PD-EAM optical gate device

barriers (6nm thick, 0.3% compressive strain). Using tensile strain wells decreases the polarization dependence. The peak photoluminescence wavelength of the MQW is $1.50\mu\text{m}$ at room temperature. The PD structure is a simple p-i-n diode with an InGaAs absorber layer of about $0.75\mu\text{m}$. Its theoretical responsivity is $\sim 0.5\text{A/W}$ with AR-coating and $\sim 0.38\text{A/W}$ without AR-coating, and a thicker absorber layer enhances responsivity.

The p-contact is obtained by depositing a Au/Zn alloy before etching the mesa shape, and the clean semiconductor surface ensures a low ohmic contact resistance. The $0.75\mu\text{m}$ $\text{In}_{0.53}\text{Ga}_{0.47}\text{As}$ absorption layer is adopted for the PD, so that the PD mesa and EAM ridge waveguide can be formed at the same time by RIE etching with CH_4/H_2 mixture gases. The next step is the traditional n-contact preparation, passivation using polymide, Ni/Cr thin film resistor deposition, and electrode process. It is necessary to clean the sidewalls of the PD and EAM before passivation to reduce dark current. After treating the surface with $1:1:50$ ($\text{H}_2\text{SO}_4 : \text{H}_2\text{O}_2 : \text{H}_2\text{O}$)^[8], dark current of PD can be dramatically reduced to about 10nA at 5V . The $\sim 250\text{nm}$ SiO_2 is deposited as AR-coating to enhance PD responsivity. The ring sharp p-electrode is formed by lithography. After cleaning the wafer, both facets of the EAM are antireflection coated.

4 Fabricated device characteristics

4.1 DC testing

PD shows excellent I - V characteristics with about 4Ω resistance and over 18V breakdown voltage. The dark current is below 10nA at 5V reverse bias. The DC responsivity is $\sim 0.32\text{A/W}$ without coating and $\sim 0.43\text{A/W}$ with SiO_2 coating, which is close to theoretical calculation. EAM also shows good I - V characteristics with $\sim 5\Omega$ resistance and over 8V breakdown voltage. The DC extinction ratio curve is shown in Fig. 4. An ER of more than 16dB is obtained

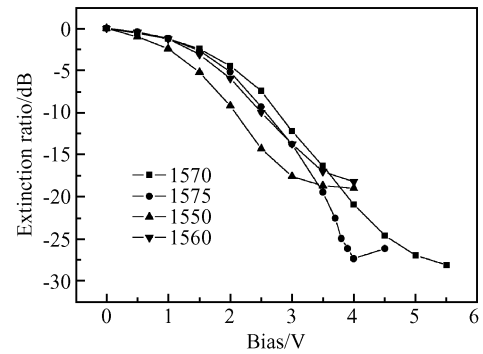


Fig. 5 Relative fiber-to-fiber ER characteristics for various wavelengths

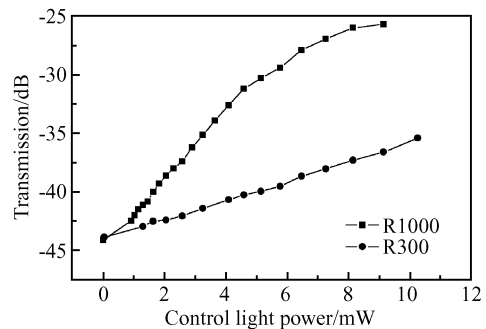


Fig. 6 PD-EAM transmission ratio versus control light

for voltage swing from 1.5V to 3.5V . The low ohmic contact resistance is achieved due to the p-contact process before etching the mesa.

Figure 6 shows the logic “and” function of the PD-EAM with 330Ω and 1000Ω load resistors. DC biases of the EAM and PD are 4.2V and 5V , respectively. The transmission loss of the PD-EAM increases $\sim 3\text{dB}$ when the power of the control light increases 1mW , and gradually saturates when the power of the control light is larger than 4mW with $R_L = 1000\Omega$. The ER is more than 18dB for a control power of 10mW . The transmission loss linearly increases $\sim 8.5\text{dB}$ with 330Ω R_L when the control light power increases to 10mW . This increase is much slower than that at 1000Ω R_L , which shows that a smaller R_L requires a higher powered control light. The DC optical “and” gate function of the PD-EAM device is demonstrated.

The capacitances of the PD and EAM are both $\sim 0.6\text{pF}$ by C - V testing. Device bandwidth can be estimated through Eq. (2). For $R_L = 950\Omega$, the bandwidth is about 500MHz . Decreasing R_L to 400Ω , the bandwidth reaches 1.25GHz .

4.2 Dynamic characteristics testing

Figure 7 shows the experimental setup for 622Mbit/s wavelength conversion with the PD-EAM. A continuous light at 1567nm generated by tunable la-

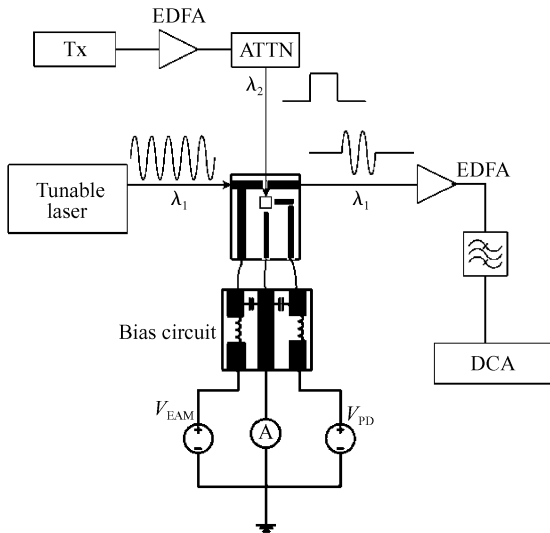


Fig.7 Experimental setup for 622Mbit/s wavelength conversion using PD-EAM

ser is coupled into the EAM. A 622Mbit/s non-return-to-zero (NRZ) pseudo random bit sequence (PRBS) optical data signal at 1550nm prepared by Anritsu ME3520A (pattern length: $2^7 - 1$) serves as the control light. It is fed into the PD after amplification by the EDFA. The output data signal light is coupled into the digital component analyzer (DCA) after amplifying and filtering.

In the setup, bias circuit is used as the DC-bias for the PD and EAM to confine the high-speed signal in the device's chip. The bias circuit contains two RF capacitors and two RF inductors on a ceramic plate. The ceramic plate is adhered by the side of the PD-EAM chip, so electrodes of PD and EAM can be connected to the bias circuit through the short golden threads to decrease electrical loss.

The testing conditions were: a DC bias of the PD and EAM of 5.2V and 4.4V, a load resistance of 950Ω , a power of continuous light of 3.5dBm, and a R_o of about 3000Ω by the relation between bias voltage and photocurrent. The measured insertion loss of the EAM is $\sim 18\text{dB}$ due to faulty alignment. The eye-diagram is shown in Fig. 8 and the control light power is adjusted to $\sim 7\text{mW}$. The eyes open clearly and the dynamic extinction ratio is $\sim 7.1\text{dB}$. The signal to noise ratio (SNR) is $\sim 5.7\text{dB}$ due to a larger insertion loss. Thus, we have successfully performed wavelength

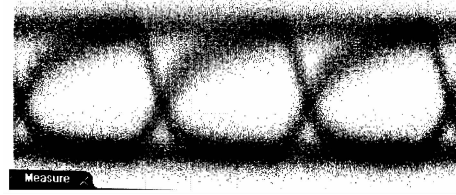


Fig.8 Eye diagram of output (wavelength conversion) signals using PD-EAM

conversion from 1550nm to 1567nm in a 622Mb/s system.

5 Conclusion

A PD-EAM optical gate on Fe-InP substrate has been successfully fabricated for the first time in China. The device shows an excellent DC logic "and" function and can be used as a wavelength converter. A dynamic extinction of over 7dB is obtained with a 950Ω load resistor and a 7mW control light power at 622Mbit/s. The principle and design guideline of the devices also have been analyzed, which shows that the bandwidth can be improved to 2.5GHz by decreasing the load resistor and capacitance of the EAM.

References

- [1] Poustie A. SOA-based all-optical processing. OFC, 2007, OHW1
- [2] Kodama S, Yoshimatsu T, Ito H. 500Gbit/s optical gate monolithically integrating photodiode and electroabsorption modulator. Electron Lett, 2004, 40(9): 555
- [3] Yoshimatsu T, Kodama S, Yoshino K, et al. 100Gbit/s error-free retiming operation of monolithic optical gate integrating with photodiode and electroabsorption modulator. Electron Lett, 2004, 40(10): 626
- [4] Kodama S, Shimizu T, Yoshimatsu T, et al. Ultrafast optical sampling gate monolithically integrating a PD and EAM. Electron Lett, 2004, 40(11): 696
- [5] Yoshimatsu T, Kodama S, Yoshino K, et al. 100-Gb/s error-free wavelength conversion with a monolithic optical gate integrating a photodiode and electroabsorption modulator. Photonic technology Lett, 2005, 17(11): 2367
- [6] Fidaner O, Demir H V, Sabnis V A, et al. Integrated photonic switches for nanosecond packet-switched optical wavelength conversion. Optical Express, 2006, 14: 361
- [7] Kang Y S, Kim S B, Chung Y D, et al. Low insertion loss electroabsorption modulator based on dual waveguide structure with spot size converter. LEOS, 2005: 422
- [8] Stocker H J, Aspnes D E. Surface chemical reactions on $\text{In}_{0.53}\text{Ga}_{0.47}\text{As}$. Appl Phys Lett, 1983, 42(1): 85

单片集成探测器和电吸收调制器光逻辑门*

廖裁宜[†] 潘教青 周 帆 边 静 朱红亮 赵玲娟 王 圩

(中国科学院半导体研究所 半导体材料重点实验室, 北京 100083)

摘要: 通过在 InP 基上单片集成光探测器和调制器, 制作了三端光逻辑门. 在不同的负载电阻下, 器件显示了良好的“与”门功能. 对芯片进行了 622MHz 的动态测试; 在 950Ω 负载条件下, 只需要约 7mW 的控制光功率即可获得大于 7dB 的动态消光比.

关键词: 电吸收调制器; 光探测器; 单片集成

EEACC: 4150; 4180; 4270

中图分类号: TN491

文献标识码: A

文章编号: 0253-4177(2008)05-0898-05

* 国家自然科学基金资助项目(批准号:90401025)

[†] 通信作者. Email: lzy1348@semi.ac.cn

2007-09-04 收到, 2007-11-17 定稿